A new self-healing epoxy with tungsten (VI) chloride catalyst

Jason M. Kamphaus[1],[*], Joseph D. Rule[2],[†], Jeffrey S. Moore[2],
Nancy R. Sottos[3] and Scott R. White[1]

[1]*Department of Aerospace Engineering,* [2]*Department of Chemistry, and*
[3]*Department of Materials Science and Engineering and The Beckman Institute for Advanced
Science and Technology, University of Illinois, Urbana, IL 61801, USA*

Using self-healing materials in commercial applications requires healing chemistry that is cost-effective, widely available and tolerant of moderate temperature excursions. We investigate the use of tungsten (VI) chloride as a catalyst precursor for the ring-opening metathesis polymerization of *exo*-dicyclopentadiene (*exo*-DCPD) in self-healing applications as a means to achieve these goals. The environmental stability of WCl_6 using three different delivery methods was evaluated and the associated healing performance was assessed following fracture toughness recovery protocols. Both as-received and recrystallized forms of the WCl_6 resulted in nearly complete fracture recovery in self-activated tests, where healing agent is manually injected into the crack plane, at 12 wt% WCl_6 loading. *In situ* healing using 15 wt% microcapsules of the *exo*-DCPD produced healing efficiencies of approximately 20%.

Keywords: tungsten (VI) chloride; ring-opening metathesis polymerization;
exo-dicyclopentadiene; self-healing

1. INTRODUCTION

Self-healing materials are inspired by many biological examples in which the healing process is triggered, regulated and completed in an autonomic fashion. For structural applications, the healing of bone (Fratzl 2007) serves as a rich source of concepts of functional adaptation in response to damage and stress state. How these concepts are being integrated in synthetic materials was also the subject of a recent special issue on this topic (Sottos *et al.* 2007).

Several techniques for achieving self-healing functionality in polymer materials have been demonstrated. These approaches include the incorporation of microcapsules (White *et al.* 2001) or hollow glass fibres containing healing agent (Pang & Bond 2005); the use of a microvascular network to deliver healing agent throughout a structure (Toohey *et al.* in press); using reversible cross-linking to induce mending after heating via molecular linkages (Chen *et al.* 2002); and a phase-separated system based on polydimethylsiloxane (Cho *et al.* 2006). Self-healing occurs when monomer is released and initiated by an embedded catalyst phase (White *et al.* 2001; Toohey *et al.* in press) or when a two-part resin system is released simultaneously in the crack plane (Pang & Bond 2005). Healing efficiencies of over 90% have been achieved for *in situ* samples with a healing chemistry that uses benzylidene-bis(tricyclohexylphosphine)dichlororuthenium (Grubbs' catalyst)

to initiate ring-opening metathesis polymerization (ROMP) of the *endo* isomer of dicyclopentadiene (DCPD; Brown *et al.* 2002). Mauldin *et al.* (2007) explored ROMP using the *exo* isomer of DCPD and Grubbs' catalyst and found that healing reached steady state approximately 20 times faster when compared with *endo*-DCPD, but at the expense of a maximum achievable healing efficiency (approximately 60% of that reached for the *endo*-DCPD). Although Grubbs' catalyst has a nearly ideal chemical selectivity, its high cost, restricted availability and limited temperature stability preclude its use in high volume, commercial composite and polymeric parts.

Alternative catalyst precursors for ROMP healing have been surveyed (Rule 2005), and tungsten (VI) chloride (WCl_6) with a co-activator was identified to have the greatest potential to address many of the limitations previously indicated. WCl_6 is a cost-effective alternative that is widely available and has a melting point of $T_m = 275°C$, which is significantly higher than that of Grubbs' catalyst ($T_m = 153°C$). The commercial potential of this class of tungsten catalyst systems has been demonstrated in the Metton (Metton America, Inc.) liquid moulding two-part resin system based on the ROMP of *endo*-DCPD (Breslow 1990).

In catalyst systems based on WCl_6, the WCl_6 itself is not the active catalyst, but rather a catalyst precursor. A key step in forming an active catalyst is the alkylation of the tungsten, and this is usually accomplished by the addition of a separate co-activator. In controlled environments (i.e. no air or impurities are present), the most effective co-activators are aggressive

*Author for correspondence (kamphaus@gmail.com).
†Present address: 3M Corporate Research Laboratory, 3M Center Building 0201-03-N-04, St Paul, MN 55144-1000, USA.

alkylating agents such as organoaluminium compounds (Breslow 1990), but they are also extremely sensitive to air and other impurities. This sensitivity makes them inappropriate for self-healing in an air environment. Therefore, as a more stable alkylating agent, we chose to use phenylacetylene, which has been shown to be an effective co-activator with WCl_6 even in air (Katz & Han 1982). In formulating this self-healing system, we also include nonylphenol as a dissolution agent (Breslow 1990). This component is necessary because self-healing is triggered by the dissolution of the catalyst into the healing agent (DCPD), and without nonylphenol, WCl_6 is nearly insoluble in DCPD.

It is also worth noting that the air environment of the self-healing reaction is expected to affect the WCl_6. A probable initial oxidation product is $WOCl_4$, which is also a ROMP-active catalyst (Balcar *et al.* 1992). Furthermore, $WOCl_4$ has been claimed to be a necessary component (in addition to the WCl_6) for effective catalysis (Breslow 1990). Therefore, for the purpose of this work, we consider both WCl_6 and any $WOCl_4$ generated by oxidation to be active catalyst precursors.

We report on the viability of WCl_6 as a ROMP active catalyst precursor for self-healing polymers. Environmental stability of this catalyst precursor was evaluated using UV-visible (UV-vis) absorbance spectrophotometry with three different WCl_6 delivery methods. The healing performance associated with each delivery method was evaluated by fracture experiments. The use of a coupling agent to increase the virgin (initial) fracture toughness was explored, as well as the effect of WCl_6 dispersion and concentration on healing performance.

2. MATERIAL AND METHODS

2.1. WCl_6 delivery methods

WCl_6 is sensitive to both moisture and the processing environment of curing epoxy resins (Rule 2005). In addition to as-received WCl_6 (Aldrich), recrystallized and a wax-protected form of WCl_6 were prepared for use in self-healing epoxy. The morphology of as-received WCl_6 is shown in figure 1*a*. The average particle sizes determined by analysis of scanning electron microscope (SEM) images for all three delivery methods are listed in table 1.

The recrystallized and wax-protected WCl_6 were prepared in a nitrogen-filled glove box or using standard Schlenk techniques (Shriver & Drezdzon 1986). Recrystallized WCl_6 was prepared according to the procedure outlined by Ketelaar & van Oosterhout (1943). WCl_6 (18.0 g) was placed in a sealed heavy-walled flask with 200 ml of dry CCl_4 (Aldrich) and heated to 120°C in an oil bath. After 30 min, heating was stopped and the sample was left to cool slowly. The resulting mixture was filtered and the WCl_6 particles were dried under vacuum. The product was then sieved and particles smaller than 180 μm were used for chemical and mechanical testing. Recrystallized WCl_6 morphology (figure 1*b*) shows a high aspect ratio planar geometry, in contrast to the as-received form. The crystal structures of both the as-received and
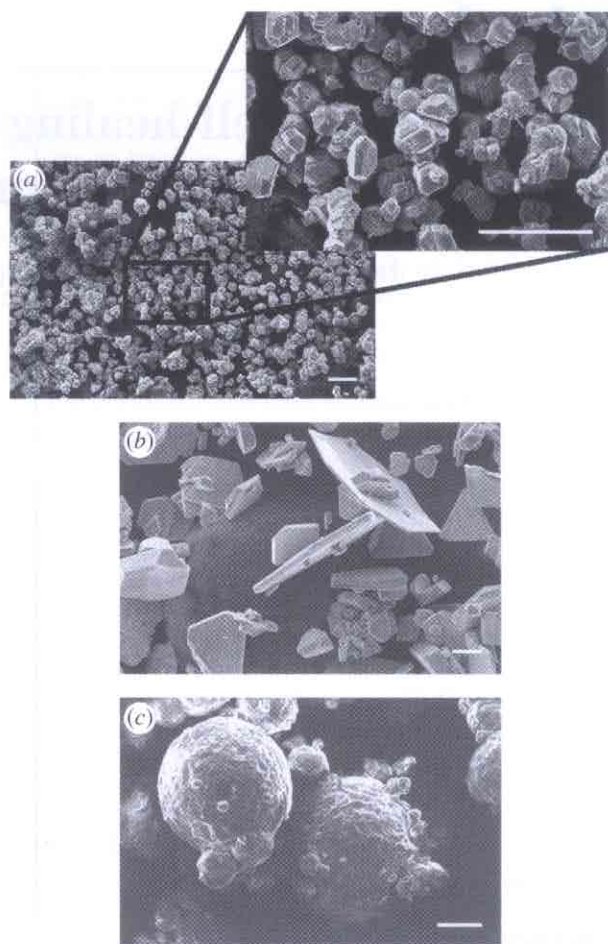
Figure 1. SEM images of WCl_6: (*a*) as-received, (*b*) recrystallized and (*c*) wax protected. (Scale bars, 100 μm.)

Table 1. Size distributions for WCl_6 delivery methods.

WCl_6 delivery method	mean size (μm)	s.d. (μm)	area/ volume (μm^{-1})
as-received	27.8	7.9	0.21
recrystallized	61.8 (planar)	43.6	0.22
	11.8 (thickness)	7.0	
wax protected	103.2	56.5	0.06

recrystallized WCl_6 were confirmed by X-ray diffraction to be the hexagonal α-WCl_6 polymorph (Ketelaar & van Oosterhout 1943).

A third delivery method was investigated in which the as-received WCl_6 was dissolved and dispersed in a paraffin wax bead in order to provide protection from potential deactivation by amines during curing of the epoxy matrix. A similar protection scheme was used by Rule *et al.* (2005) for Grubbs' catalyst. WCl_6 (5.25 g) was added to a 40 ml vial with 730 mg of the dissolution agent nonylphenol (Aldrich) and 9.0 g of paraffin wax (melting point of 58–62°C, Aldrich). The dissolution agent was added to compatibilize the WCl_6 with the wax beads and to facilitate dissolution in the DCPD healing agent. The vial was capped and placed in a 120°C bath and magnetically stirred. In a separate bath, 300 ml of dry perfluorodecalin (Flutec PP6, F2 Chemicals) was stirred at 1250 r.p.m. with a mechanical

mixer in a 1000 ml beaker until it reached a temperature of 65°C. Upon complete melting of the wax, the sample mixture was poured into the perfluorodecalin bath and allowed to stir for 1 min. Approximately 700 ml of chilled perfluorodecalin was quickly added to the hot perfluorodecalin bath to quench the suspension and solidify the wax beads. The perfluorodecalin and wax mixture was vacuum filtered and the wax beads (figure 1c) were dried under vacuum. The beads were then sieved and the beads smaller than 355 µm were kept for further study. Elemental analysis of the wax beads revealed that the concentration of tungsten was 10 wt%, while the theoretical tungsten concentration based on the mixture ratio was 16%. After processing, a dense solid remained in the vial suggesting incomplete dissolution of the WCl_6 had occurred.

2.2. Assessment of environmental stability

Environmental stability of the three forms of WCl_6 was monitored using UV-visible absorbance spectrophotometry. Samples exposed to air (22°C, 30% relative humidity) for 0, 2 or 24 h were brought into an argon-filled glove box and dissolved in dry toluene at a concentration of 0.8 mM of tungsten. The UV-vis absorbance spectra were taken at wavelengths from 280 to 800 nm in quartz cuvettes (path length of 0.1 cm) with Teflon seals.

2.3. Sample preparation

Tapered double-cantilever beam (TDCB) fracture specimens (Brown *et al.* 2002) were adopted to evaluate healing performance. The tapered geometry allows for a crack length-independent fracture toughness measurement. Localized TDCB specimens, as shown in figure 2, were manufactured using Epon 828 epoxy resin (Miller-Stephenson) cured with 12 pph Ancamine DETA (Air Products). Since the crack is directed along the centreline of the specimens, only the material near the centreline is used during self-healing. Therefore, the sample was made in two stages such that only the material near the centreline possesses self-healing functionality. A method developed by Rule *et al.* (2007) was used in which a non-self-healing blank was formed in the outer regions of the TDCB geometry by pouring neat resin epoxy into a silicon rubber mould that contained a 7 mm wide insert around the grooved section of the sample. The blanks used for *in situ* samples also contained microcapsules at the same concentration as the centre material. Rule *et al.* (2007) found that the measured fracture toughness was artificially high for *in situ* samples with no capsules in the blank. However, by incorporating the same concentration of microcapsules in the blank, the modulus and thermal expansion coefficient are matched with the self-healing centre and accurate fracture toughness data are obtained. The blank was then cured for 24 h at 22°C.

The insert was subsequently removed and the self-healing material was prepared for the second stage of specimen manufacturing. Two types of samples were fabricated: self-activated and *in situ*. Self-activated
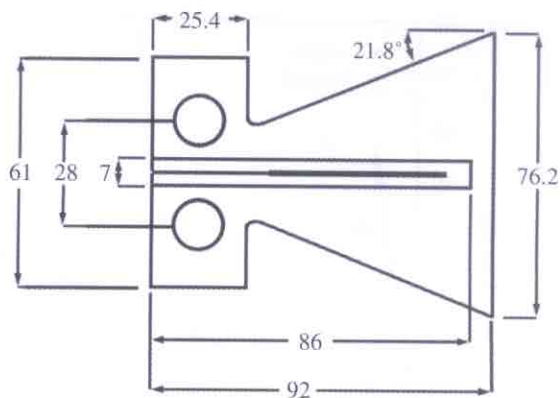

Figure 2. Localized TDCB specimen geometry (all dimensions in millimetres; Rule *et al.* 2007).

samples contained WCl_6, but no healing agent and *in situ* samples contained both WCl_6 and microencapsulated DCPD (Brown *et al.* 2002). Epoxy resin was degassed and allowed to react for 30 min prior to the addition of WCl_6 to permit time for the viscosity of the resin to increase (preventing settling of WCl_6 particles) and reduce the concentration of free amines. The desired amount of WCl_6 was then added to the epoxy resin. Higher concentrations of wax-encapsulated WCl_6 (more than 20 wt%) were not possible due to excessive viscosity of the resin mixture. Unless otherwise stated, samples were mixed by hand. The effect of WCl_6 dispersion was investigated by comparing hand-mixed and mechanically mixed samples.

For *in situ* self-healing samples, microcapsules were also added to the mixture at this time. These microcapsules contained *exo*-DCPD, phenylacetylene (45 mM) and nonylphenol (45 mM) and were manufactured by an established interfacial polymerization encapsulation technique (Brown *et al.* 2003). The resulting capsules were sieved and the distribution used for analysis was 188 ± 31 µm. The resin mixture was then poured into the centre of the blank and the mould was closed. All samples were cured for 24 h at 22°C followed by an additional 24 h at 35°C. The samples were removed from the moulds, allowed to cool to 22°C and then tested.

2.4. Mechanical assessment of healing performance

TDCB fracture specimens were similar to those used by Rule *et al.* (2007), but with a nominal crack width of 3.8 mm and an overall specimen thickness of 7.1 mm. The fracture toughness is determined as

$$K_{I_c} = \alpha P_c, \qquad (2.1)$$

where P_c is the critical fracture load and α is a scaling parameter that depends on the specimen geometry and material properties and is equal to 8777 m$^{-3/2}$, which was calculated from Brown *et al.* (2002) data for the thicker samples used here. The healing efficiency was calculated as

$$\eta = \frac{K_c^{\text{healed}}}{K_c^{\text{virgin}}} = \frac{P_c^{\text{healed}}}{P_c^{\text{virgin}}}, \qquad (2.2)$$
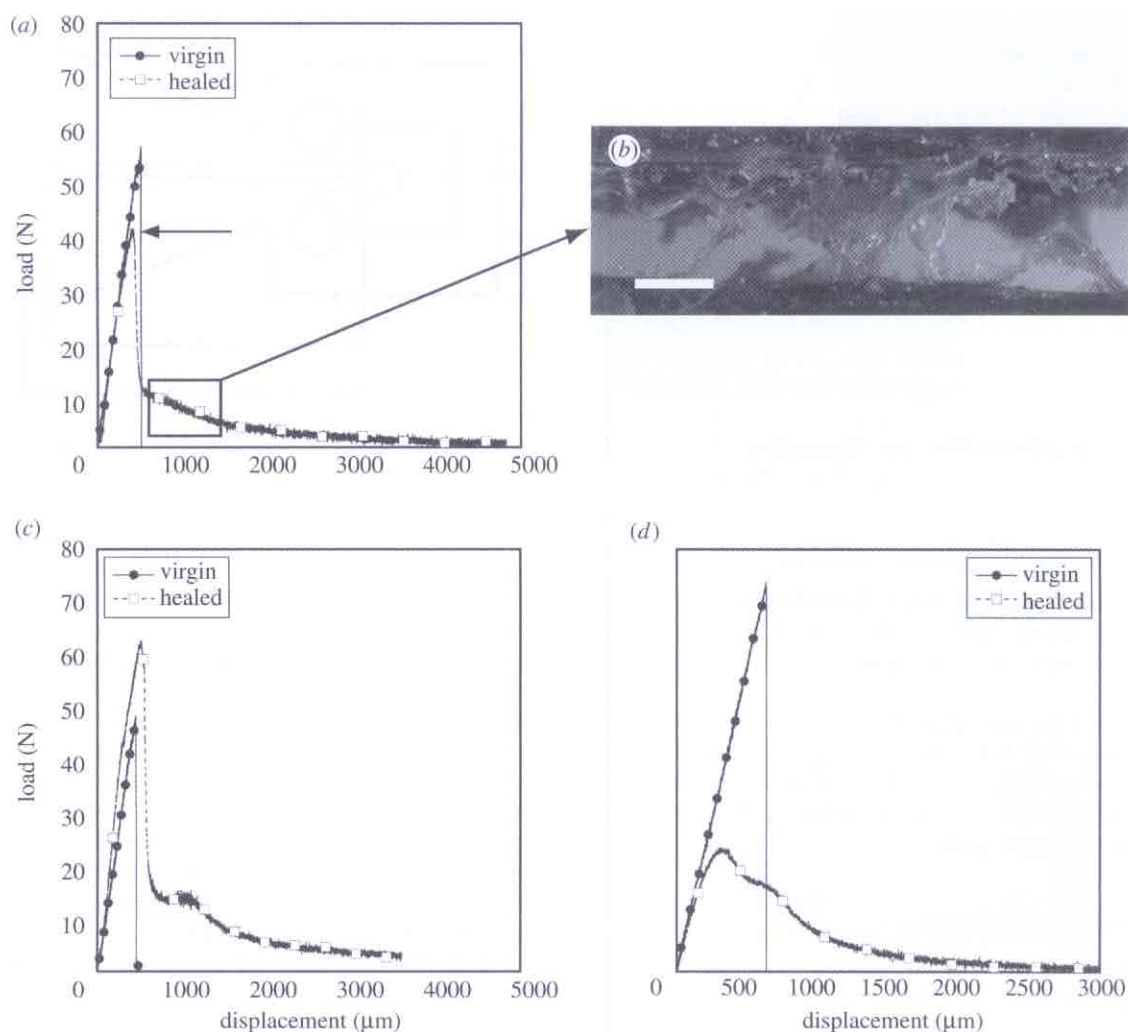
Figure 3. Mechanical assessment of self-activated specimens. (*a*) Representative load versus displacement data for recrystallized specimens (arrow indicates the peak of the healed response). (*b*) Image of poly(DCPD) fibrils spanning the fracture plane (scale bar, 1 mm). (*c*) Representative load versus displacement data for as-received specimens. (*d*) Representative load versus displacement data for wax-protected samples.

where P_c^{virgin} is the critical fracture load of the initial fracture and P_c^{healed} is the critical fracture load after healing.

Some samples exhibited a nonlinear response after healing. These experiments were analysed using a method outlined by Rule *et al.* (2005) which defines an alternative healing efficiency as

$$\eta' = \frac{A_{\text{healed}}/b_n\left(W - a_0^{\text{healed}}\right)}{A_{\text{virgin}}/b_n\left(W - a_0^{\text{virgin}}\right)}, \qquad (2.3)$$

where A is the total area under the load–displacement curve; b_n is the width of the crack plane (3.8 mm); W is the distance from the centre of the loading pins to the end of the specimen (79.3 mm); a_0^{virgin} is the initial crack length for the virgin test; and a_0^{healed} is the initial crack length for the healed test. Both η (the recovery of the linear-elastic fracture toughness) and η' (the recovery of the total fracture energy) are independent measures of healing efficiency and they cannot be directly compared.

The testing of the TDCB samples followed previously established protocols for self-activated samples where the samples contain the catalyst phase and the healing agent is manually injected into the crack (Brown *et al.* 2002).

A small starter crack was initiated by tapping a razor blade into a moulded starter notch. The samples were pin loaded in Mode I using displacement control at 5 μm s^{-1} until complete failure. After the virgin (initial) test, the two pieces of the sample were brought back together in alignment while maintaining a small gap of approximately 1 mm between the crack faces. Approximately 100 μl of a healing solution was then injected between the crack faces. For samples containing wax-protected WCl$_6$, the healing solution was prepared by mixing 5 μl of phenylacetylene (Aldrich) and 1 ml of *exo*-DCPD synthesized from *endo*-DCPD (Acros) (Nelson & Kuo 1975). For samples containing as-received or recrystallized WCl$_6$, 10 mg of nonylphenol, a dissolution agent, was added to the above-mentioned healing solution. The nonylphenol was omitted from the healing solution for wax-protected WCl$_6$, as it is already present in the wax beads. Once the healing solution was injected, the crack faces were then brought into full contact and left undisturbed for 48 h. After healing, the samples were tested again without initiating another starter crack. Figure 3*a*,*c* and *d* show typical load versus displacement plots for self-activated recrystallized, as-received and

wax-encapsulated delivery methods. For the as-received and recrystallized samples, a two-stage failure process was observed. Healed specimens exhibited an initial linear elastic response until reaching a critical fracture load after which a precipitous drop in load-carrying capability was observed. Continued deformation of the samples leads to a lengthy and gradual decline in load and a ductile-type failure mode that absorbs a significant amount of energy before final failure is achieved. During this second ductile failure stage, partially polymerized poly(DCPD) fibrils that bridge the crack plane provide a means of load transfer between the two halves of the sample (figure 3*b*).

In situ samples were tested in a similar fashion to the self-activated samples, but no additional healing agent was manually applied in these cases. Rather, healing agent delivery is accomplished autonomically via fracture of microcapsules contained within the sample.

3. RESULTS

3.1. Environmental stability of WCl₆

Figure 4 shows the UV-vis spectra for the different WCl_6 forms investigated. The initial spectra for the as-received and recrystallized compound are consistent with published results (Thorn-Csányi & Timm 1985). After exposure to ambient air for 2 h, about half of the as-received WCl_6 remains, while the recrystallized WCl_6 has been completely converted to either $WOCl_4$ (as evidenced by the single peak at 355 nm reported by Thorn-Csányi & Timm (1985)) or other non-absorbing or insoluble compounds. The spectra for the wax-protected WCl_6 are qualitatively different with a significant absorption band above 500 nm. Complexes of WCl_6 with phenols have been reported to have similar absorption spectra (Balcar *et al.* 1992), so this suggests that the tungsten in the wax-protected catalyst exists as a complex with the nonylphenol that is added. The as-received WCl_6 retained some presumably active $WOCl_4$ after 24 h of exposure, while the recrystallized and wax-encapsulated forms retained no WCl_6 or $WOCl_4$.

3.2. Healing of the self-activated system

Self-activated tests were performed to demonstrate and refine the system. Specifically they were used to evaluate the effect of (i) WCl_6 delivery methods, (ii) a coupling agent on the virgin toughness, and (iii) the dispersion of the WCl_6 on the self-healing performance. Table 2 summarizes the results of these experiments.

3.3. Effect of WCl₆ delivery methods

Self-activated TDCB specimens with 4.4, 7 or 12 wt% of as-received or recrystallized WCl_6 were tested. The virgin and the initial portion of the healed load–displacement data for the 7 and 12 wt% samples were linear (figure 3*a,b*) and therefore satisfied the requirements for the use of equation (2.2). To account for the large amount of energy consumed in the second stage of failure of these samples, we also calculated healing
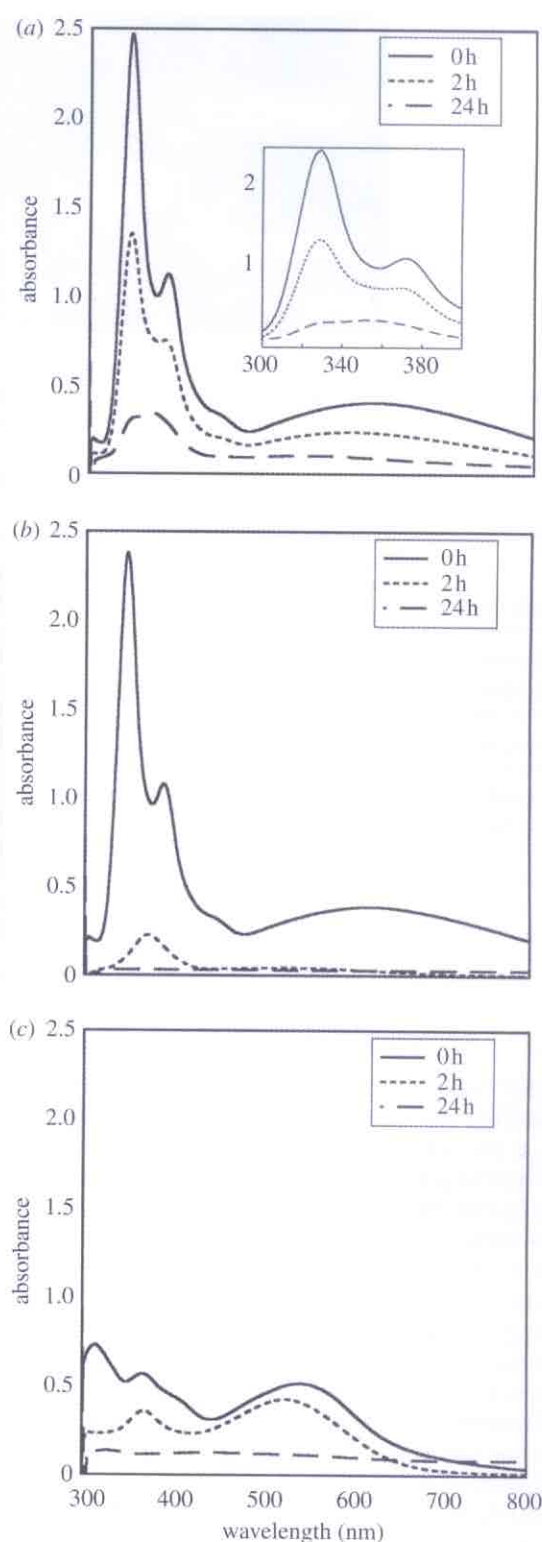

Figure 4. UV-vis spectra results for (*a*) as-received with inset of spectra from 300 to 400 nm, (*b*) recrystallized and (*c*) wax-protected WCl_6 upon exposure to air at 22°C and 30% relative humidity for 0, 2 and 24 h. The characteristic peaks for WCl_6 are located at 328 and 372 nm and for $WOCl_4$ at 355 nm (Thorn-Csányi & Timm 1985).

efficiencies using equation (2.3) for all sample types. The 4.4 wt% samples containing recrystallized WCl_6 and a coupling agent exhibited a nonlinear healing response; therefore, equation (2.3) was used to quantify the healing efficiency. The polymerized healing agent was removed from the crack plane and analysed by
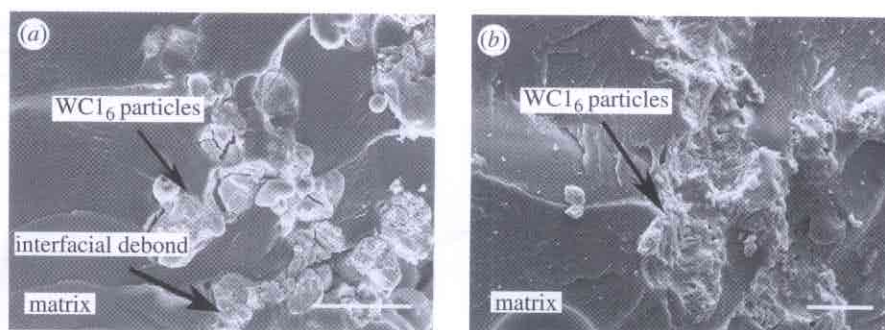
Figure 5. SEM images of epoxy fracture surfaces for samples containing as-received WCl_6 (12 wt%). (*a*) Significant interfacial debonding is revealed when no coupling agent is used. (*b*) The addition of 1 wt% silane coupling agent (3-glycidoxypropyltrimethoxysilane) dramatically reduces the amount of interfacial debonding (scale bars, 50 μm).

Table 2. Summary of healing efficiencies for the three WCl_6 delivery methods and the effect of coupling agent on fracture toughness.

sample type	no. of samples	WCl_6 loading (wt%)	coupling agent (wt%)	$K_{I_c}^{\text{virgin}}$ (MPa·m$^{1/2}$)	$K_{I_c}^{\text{healed}}$ (MPa·m$^{1/2}$)	η (%)	η' (%)
neat resin	8	0	0	0.84 ± 0.06	—	—	—
neat resin	8	0	1	0.85 ± 0.08	—	—	—
as-received	5	7	0	0.44 ± 0.11	0.20 ± 0.09	46	187
as-received	6	12	0	0.44 ± 0.03	0.47 ± 0.07	107	263
as-received	4	12	1	0.67 ± 0.14	0.52 ± 0.14	78	247
recrystallized	7	4.4	1	0.55 ± 0.10	NL[b]	—	11
recrystallized	4	7	0	0.37 ± 0.04	0.17 ± 0.04	46	160
recrystallized	7	12	0	0.41 ± 0.06	0.37 ± 0.12	90	231
recrystallized	5	12	1	0.66 ± 0.09	0.44 ± 0.09	67	204
wax protected[a]	4	4.4	0	0.60 ± 0.05	NL[b]	—	49
in situ[c]	3	12	0	0.85 ± 0.06	NL[b]	—	20

[a] 20 wt% wax beads in epoxy resin with 22 wt% WCl_6 concentration in wax.
[b] NL, nonlinear healing response.
[c] 15 wt% microcapsules of *exo*-DCPD/phenylacetylene/nonylphenol.

Fourier transform infrared spectroscopy (FTIR). By monitoring the spectra and observing the characteristic peak at 965 cm^{-1} corresponding to the *trans* double bond for both the polymerized healing agent and an authentic poly(*exo*-DCPD) control, it was confirmed that the achieved healing was a result of ROMP of *exo*-DCPD.

Self-activated TDCB samples containing 20 wt% of wax-encapsulated WCl_6 (4.4 wt% overall catalyst loading) were also evaluated. A nonlinear healing response (figure 3*c*) was obtained and the healing efficiency was evaluated using equation (2.3). The nonlinearity upon healing in this case is probably due to either plasticization of the healed poly(DCPD) film by dissolved wax (Rule *et al.* 2007) or to incomplete polymerization as a result of the lower effective catalyst concentration as was exhibited in the 4.4 wt% recrystallized catalyst samples.

3.4. Effect of coupling agent

A decrease in the virgin fracture toughness was observed for both the as-received and recrystallized WCl_6 samples as shown in table 2. In both cases, regardless of WCl_6 concentration, a large (approximately 50%) decrease in virgin fracture toughness occurs when compared with neat resin. The size, shape, concentration and bonding of the particles to the matrix were all considered as possible causes for the decrease in toughness, but poor interfacial

bonding between the WCl_6 and epoxy matrix was thought to be the prevailing effect. There is precedence in the literature for a decrease in fracture toughness of polymers due to poor adhesion of inclusions (Maiti & Sharma 1992; Wong & Truss 1994; Brown *et al.* 2004). Other factors such as particle shape, size, volume fraction and distribution may also decrease toughness (Lange & Radford 1971; Quazi *et al.* 1999) and may account for the difference between the neat resin samples and the WCl_6 samples containing coupling agent.

To confirm that poor interfacial bonding between the WCl_6 and matrix was the dominant cause of decreased fracture toughness, a series of experiments were carried out with and without adhesion promoter. During manufacturing, 1 wt% of the silane coupling agent 3-glycidoxypropyltrimethoxysilane (Aldrich) was added to the epoxy resin prior to addition of the WCl_6 phase. A series of control samples with 1 wt% coupling agent, but no WCl_6 phase, were also tested.

Control experiments confirmed that the addition of coupling agent has no effect on the fracture toughness of the neat epoxy. More importantly, the addition of the coupling agent increased the toughness of the as-received and recrystallized WCl_6 samples almost to levels consistent with the neat epoxy samples. Scanning electron images comparing the fracture surfaces of samples with and without coupling agent are shown in figure 5. Debonding between the WCl_6 and matrix
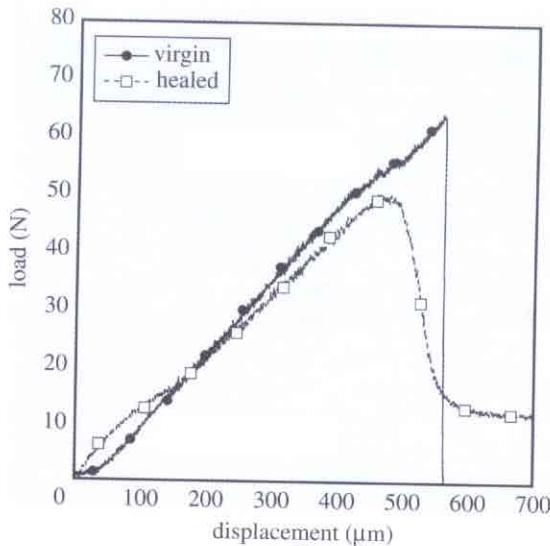
Figure 6. Self-activated mechanical response of a sample containing 12 wt% recrystallized WCl$_6$ with 1 wt% coupling agent in the matrix.
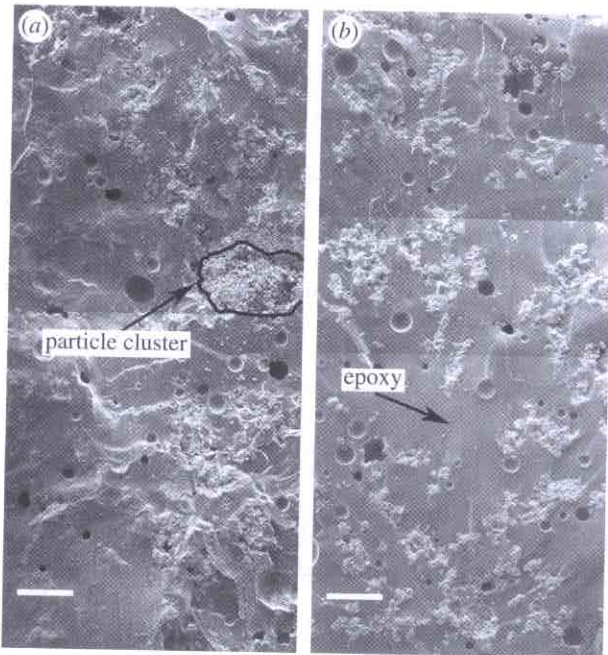

Figure 7. SEM images of epoxy fracture surfaces for samples containing as-received WCl$_6$ (12 wt%). (*a*) Significant clustering of tungsten particles in the absence of mechanical mixing. (*b*) Particle dispersion achieved by mechanical mixing at 500 r.p.m. (scale bars, 500 µm).

phase is clearly evident in the sample without coupling agent and it is dramatically suppressed when the coupling agent is added. A subset of the self-activated samples containing coupling agent was tested and a representative load versus displacement response for these samples is shown in figure 6. The healing for both types of WCl$_6$ delivery was unaffected by the addition of the coupling agent, as shown in table 2.

3.5. Effect of dispersion

The as-received form of the WCl$_6$ has a tendency to agglomerate into large particle clusters in the epoxy resin during processing and the lack of uniform dispersion
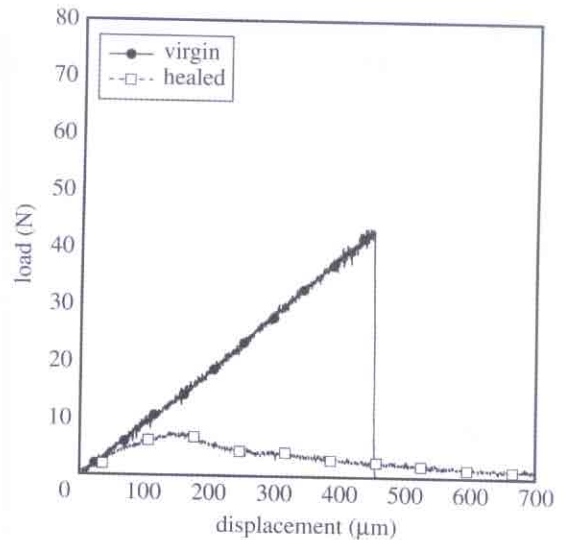

Figure 8. Self-activated mechanical response of a sample containing 12 wt% as-received WCl$_6$ dispersed with mechanical mixing at 500 r.p.m.

Table 3. Summary of cluster parameters of samples with and without mechanical mixing.

sample type	$\bar{r}$ (µm)	σ^2 (µm^2)	Q	R
random distribution[a]	149.4	6100.8	1.00	1.00
with mechanical mixing	142.3	5659.5	0.95	0.93
random distribution[b]	147.6	5954.0	1.00	1.00
without mechanical mixing	126.1	10 387.2	0.85	1.74

[a] based on image from figure 7*a*.
[b] based on image from figure 7*b*.

leads to inconsistent healing. In order to obtain better dispersion, the as-received WCl$_6$ was incorporated in the epoxy resin using a mechanical mixer stirring at 500 r.p.m. prior to pouring into the moulds.

SEM images of samples with and without mechanical mixing are compared in figure 7. Image analysis was performed to ascertain the relative level of clustering of the WCl$_6$ particles. A method outlined by Schwarz & Exner (1983) to characterize the clustering of points was implemented. The distance from the centroid of each cluster to its nearest neighbour was calculated. The mean and variance of the distribution of distances was calculated for samples with and without mechanical mixing as well as a random distribution from a Poisson point process with the same number of particles and image size as each sample image. The parameters Q and R were calculated as

$$Q = \frac{\bar{r}_{\text{image}}}{\bar{r}_{\text{random}}} \tag{3.1}$$

and

$$R = \frac{\sigma^2_{\text{image}}}{\sigma^2_{\text{random}}}, \tag{3.2}$$

where $\bar{r}_{\text{image}}$ and $\bar{r}_{\text{random}}$ are the mean distances to nearest neighbours for the image of interest and the random distribution, respectively, and the σ^2_{image} and σ^2_{random} are the variances of the distribution of distances to nearest neighbours of the image of interest and the random distribution.
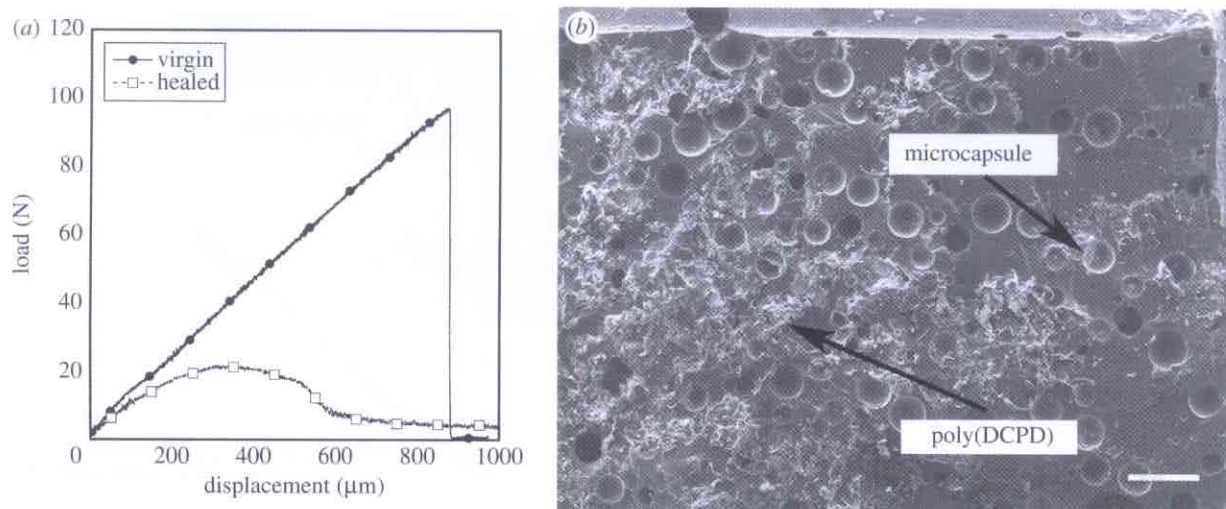
Figure 9. (*a*) *In situ* mechanical response of a sample containing 12 wt% recrystallized WCl$_6$ and 15 wt% 188±31 μm capsules and (*b*) SEM image of the fracture surface of an *in situ* sample after healing and refracture (scale bar, 500 μm).

Deviation of Q or R from unity indicates some degree of clustering and was used to characterize the relative clustering between the two mixing conditions. Table 3 summarizes the results from this analysis. Both the Q and R values for the mechanically mixed sample deviated from unity by less than 7%. When no mechanical mixing was used, image analysis yielded $Q=0.85$ and $R=1.74$, indicating significant clustering of catalyst particles. Interestingly, the healing efficiency of the well-dispersed WCl$_6$ samples dropped from 107 to 20% and the healing response was nonlinear, as shown in figure 8.

3.6. Self-healing of the in situ *microencapsulated system*

In situ healing experiments were performed with 12 wt% recrystallized WCl$_6$ and 15 wt% microcapsules that contained a healing solution of *exo*-DCPD, nonylphenol and phenylacetylene at the same concentrations as the self-activated healing solution. The healed samples exhibited a nonlinear fracture response, as shown in figure 9*a*, indicating incomplete polymerization of the poly(DCPD) film. Figure 9*b* shows a representative SEM image of the fracture surface after healing of an *in situ* sample. Broken microcapsules and poly(*exo*-DCPD) film are present on the fracture surface, indicating that mechanical triggering of the monomer release occurred. Healing efficiency calculated using equation (2.3) is 20%.

4. DISCUSSION

Self-activated TDCB experiments clearly demonstrate the effectiveness of WCl$_6$ as a catalyst precursor for self-healing epoxy. Of the delivery methods examined, the as-received morphology retains the greatest activity upon exposure to laboratory air. The surface area to volume ratio of the particles may play an important role in the environmental stability of the particles. Table 1 shows the surface area to volume ratio for each of the three WCl$_6$ forms. The as-received and recrystallized forms have similar surface areas per unit

volume, indicating that the difference in stability is not directly attributed to the surface area, but may be dictated by the smallest critical dimension. As the outer surface oxidizes, more of the WCl$_6$ remains active in the as-received particles with a larger critical dimension (27.8 μm) in comparison with the recrystallized particles with the smaller critical dimension (11.8 μm). Wax protection of the WCl$_6$ phase achieved mixed results—healing was obtained for effective WCl$_6$ concentrations that were lower than could be obtained by other delivery methods (4.4 wt%), but no healing activity could be detected after 24 h exposure to laboratory air.

Inherently coupled with the deactivation problem, dispersion of the WCl$_6$ phase within the epoxy matrix plays an important role in the efficiency of healing. Healing activity is preserved via particle clustering—presumably by sealing interior particles from exposure to the surrounding polymer matrix. When these clusters are broken up and dispersed through strong mechanical mixing, the healing efficiency dramatically decreases. Embedding the WCl$_6$ phase in wax leads to better dispersion while maintaining reasonable healing efficiency.

For the as-received and recrystallized delivery methods, more than 7 wt% WCl$_6$ loading was necessary to achieve complete healing. Some portion of the WCl$_6$ was deactivated during specimen manufacturing and curing. Hence, better protection schemes will enable lower tungsten loadings in the future. Even with the technical challenges identified, *in situ* healing was demonstrated (approx. 20%) using 12 wt% as-received WCl$_6$ and 15 wt% microcapsules containing *exo*-DCPD healing agent. More effective protection schemes for WCl$_6$ and other co-activators mixed with the healing agent are being examined for further enhancement of this self-healing system.

5. CONCLUSIONS

A cost-effective way to achieve self-healing was demonstrated using WCl$_6$ with a co-activator (phenylacetylene) that initiates ROMP of *exo*-DCPD. The environmental

stability of three WCl_6 delivery methods was investigated by UV-vis spectrophotometry and the as-received form shows the greatest stability after 24 h exposure to laboratory air. Self-activated healing of TDCB fracture specimens showed nearly complete recovery for 12 wt% catalyst loading for both as-received and recrystallized WCl_6, but strong mechanical mixing to promote dispersion of the catalyst reduced healing efficiency dramatically. The virgin fracture toughness of epoxy was reduced by approximately 48% upon addition of WCl_6 particles and this reduction was attributed to poor interfacial bonding. Incorporating a silane coupling agent into the matrix resin increased the virgin fracture toughness to approximately 75% of the neat resin toughness. Preliminary *in situ* healing experiments using 12 wt% as-received WCl_6 and 15 wt% 188 μm microcapsules containing *exo*-DCPD healing agent, 0.5 wt% phenylacetylene and 1.0 wt% nonylphenol yielded approximately 20% healing efficiency. Further research is required to optimize the healing efficiency by more effective WCl_6 protection schemes, more efficient co-activators and enhanced processing methods to achieve uniform WCl_6 dispersion.

REFERENCES

Balcar, H., Dosedlová, A. & Petrusová, L. 1992 Ring-opening metathesis polymerization of dicyclopentadiene by unicomponent catalysts derived from WCl_6. *J. Mol. Catalysis* **77**, 289–295. (doi:10.1016/0304-5102(92)80208-X)

Breslow, D. S. 1990 How we made neat stuff. *Chemtech* **20**, 540–544.

Brown, E. N., Sottos, N. R. & White, S. R. 2002 Fracture testing of a self-healing polymer composite. *Exp. Mech.* **42**, 372–379. (doi:10.1177/001448502321548193)

Brown, E. N., Kessler, M. R., Sottos, N. R. & White, S. R. 2003 *In situ* poly(urea-formaldehyde) microencapsulation of dicyclopentadiene. *J. Microencap.* **20**, 719–730. (doi:10.1080/0265204031000154160)

Brown, E. N., White, S. R. & Sottos, N. R. 2004 Microcapsule induced toughening in a self-healing polymer composite. *J. Mater. Sci.* **35**, 1703–1710. (doi:10.1023/B:JMSC.00000 16173.73733.dc)

Chen, X., Dam, M. A., Ono, K., Mal, A., Shen, H., Nutt, S. R., Sheran, K. & Wudl, F. 2002 A thermally re-mendable cross-linked polymeric material. *Science* **295**, 1698–1702. (doi:10.1126/science.1065879)

Cho, S. H., Andersson, M. H., White, S. R., Sottos, N. R. & Braun, P. V. 2006 Polydimethylsiloxane-based self-healing materials. *Adv. Mater.* **18**, 997–1000. (doi:10.1002/adma. 200501814)

Fratzl, P. 2007 Biomimetic materials research: what can we really learn from nature's structural materials? *J. R. Soc. Interface* **4**, 637–642. (doi:10.1098/rsif.2007.0218)

Katz, T. J. & Han, C. C. 1982 Induction of olefin metathesis by phenylacetylene plus tungsten hexachloride. *Organometallics* **1**, 1093–1096. (doi:10.1021/om00068a019)

Ketelaar, J. A. A. & van Oosterhout, G. W. 1943 Die krystalstruktur des wolframhexachlorids. *Recueil des Travaux Chimiques des Pays-Bas et de la Belgique* **62**, 197–200.

Lange, F. F. & Radford, K. C. 1971 Fracture energy of an epoxy composite system. *J. Mater. Sci.* **6**, 1197–1203. (doi:10.1007/BF00550203)

Maiti, S. N. & Sharma, K. K. 1992 Studies on polypropylene composites filled with talc particles. I. Mechanical properties. *J. Mater. Sci.* **27**, 4605–4613. (doi:10.1007/BF011 65994)

Mauldin, T. C., Rule, J. D., Sottos, N. R., White, S. R. & Moore, J. S. 2007 Self-healing kinetics and the stereoisomers of dicyclopentadiene. *J. R. Soc. Interface* **4**, 389–393. (doi:10.1098/rsif.2006.0200)

Nelson, G. L. & Kuo, C. L. 1975 An improved procedure for the preparation of exo-dicyclopentadiene. *Synthesis* **105**, 105–106. (doi:10.1055/s-1975-23674)

Pang, J. W. C. & Bond, I. P. 2005 A hollow fibre reinforced polymer composite encompassing self-healing and enhanced damage visibility. *Compos. Sci. Technol.* **65**, 1791–1799. (doi:10.1016/j.compscitech.2005.03.008)

Quazi, R. T., Bhattacharya, S. N. & Kosior, E. 1999 Effect of dispersed paint particles on the mechanical properties of rubber toughened polypropylene composites. *J. Mater. Sci.* **34**, 607–614. (doi:10.1023/A:1004 515300637)

Rule, J. D. 2005 Polymer chemistry for improved self-healing composite materials. PhD thesis, University of Illinois at Urbana-Champaign, Urbana, IL.

Rule, J. D., Brown, E. N., Sottos, N. R., White, S. R. & Moore, J. S. 2005 Wax-protected catalyst microspheres for efficient self-healing materials. *Adv. Mater.* **17**, 205–208. (doi:10.1002/adma.200400607)

Rule, J. D., Sottos, N. R. & White, S. R. 2007 Effect of microcapsule size on the performance of self-healing materials. *Polymer* **48**, 3520–3529. (doi:10.1016/j.polymer.2007.04.008).

Schwarz, H. & Exner, H. E. 1983 The characterization of the arrangement of feature centroids in planes and volumes. *J. Microsc.* **129**, 155–169.

Shriver, D. F. & Drezdzon, M. A. 1986 *The manipulation of air-sensitive compounds*, 2nd edn. New York, NY: Wiley-Interscience.

Sottos, N. R., White, S. R. & Bond, I. P. 2007 Self-healing polymers and composites. *Papers of a themed supplement* **4**, 347–411.

Thorn-Csányi, E. & Timm, H. 1985 Kinetic studies of the system tungsten hexachloride/tetramethyltin (diethyl ether)/C_5-olefins; determination of the initial reaction steps. *J. Mol. Catalysis* **28**, 37–48. (doi:10.1016/0304-5102(85)87016-4)

Toohey, K., Lewis, J. A., Moore, J. S., White, S. R. & Sottos, N. R. In press. Self-healing materials with microvascular networks. *Nat. Mater.*

White, S. R., Sottos, N. R., Geubelle, P. H., Moore, J. S., Kessler, M. R., Sriram, S. R., Brown, E. N. & Viswanathan, S. 2001 Autonomic healing of polymer composites. *Nature* **409**, 794–797. (doi:10.1038/35057232)

Wong, K. W. Y. & Truss, R. W. 1994 Effect of flyash content and coupling agent on the mechanical properties of flyash-filled polypropylene. *Compos. Sci. Technol.* **52**, 361–368. (doi:10.1016/0266-3538(94)90170-8)